

Orientation of Arachidate Chains in Langmuir-Blodgett Monolayers on Si(111)

D. A. Outka, J. Stöhr, J. P. Rabe, J. D. Swalen, and H. H. Rotermund

IBM Almaden Research Center, San Jose, California 95120

(Received 1 June 1987)

The near-edge x-ray-absorption fine-structure technique is used to determine the orientation of cadmium- and calcium-arachidate chains on Si(111) at monolayer coverage. In our films the Cd-arachidate chain is found to be aligned along the surface normal and Ca arachidate is tilted by $33^\circ \pm 5^\circ$ relative to Cd arachidate. The results are explained in terms of the surface bonding geometry of the terminal carboxylate group and the lateral interlocking of the zig-zag chains.

PACS numbers: 68.55.Jk, 78.70.Dm, 82.65.Jv

The interest in Langmuir-Blodgett (LB) films on surfaces arises from their potential technological importance in microlithography, electro-optics, biochemical sensing, and tribology.¹ Numerous studies have been conducted of LB films to determine the structure and orientation of the films.²⁻⁷ Because of the scarcity of nondestructive techniques sensitive to LB *monolayers* previous studies have mainly dealt with periodic multilayer films. Here we present the first application of the near-edge x-ray-absorption fine-structure (NEXAFS)⁸ technique to the study of thin organic films on surfaces. Because of its high surface sensitivity and the pronounced polarization dependence of the carbon *K*-shell spectra, NEXAFS is found to be a powerful technique for the structural investigation of LB monolayers. In particular, we accurately determine the orientation of cadmium arachidate (CdA) and calcium arachidate (CaA) $\{M[\text{CH}_3(\text{CH}_2)_{18}\text{CO}_2]\}$ ($M = \text{Cd}$ and Ca) on a Si(111) wafer. Our results are explained by a model which links particular chain orientations on the surface to the surface bonding geometry of the terminal carboxylate group and the lateral interlocking geometry of the zig-zag hydrocarbon skeleton.

The experiments were performed on beam line I-1 at the Stanford Synchrotron Radiation Laboratory with use of a grasshopper monochromator (1200-line/mm holographic grating). The NEXAFS spectra were obtained by total-electron-yield detection and normalized by the signal from a gold-grid monitor in order to correct for the transmission function of the monochromator. The x-ray incidence angle θ was varied from 10° glancing incidence (\vec{E} near surface normal) to normal incidence (\vec{E} in surface plane). Single-layer LB films were prepared on Si(111) wafers. The silicon wafer used as a substrate was stripped of its natural oxide coating with Buffered Oxide Etch. Immediately preceding the transfer of the LB monolayer, the silicon was further cleaned with a solution of No Chro Mix Water and dried in nitrogen flow. The LB monolayers were prepared on a commercially available film balance with a solid Teflon trough instead of the originally supplied glass tank. The solutions used to prepare the LB films were 2.5×10^{-4} mol

l^{-1} CdCl_2 maintained at a *pH* between 7 and 7.5 with a Na_2CO_3 buffer for CdA and 1.0×10^{-4} mol l^{-1} CaCO_3 maintained at a *pH* between 7 and 8 for CaA. The transfer pressure used was 30 mN m^{-1} . The samples were measured as prepared in a vacuum of about 1×10^{-8} Torr.

Figure 1 compares the angular dependence of the NEXAFS spectra of CdA and CaA films.⁹ The top row shows the spectra at normal incidence and the second row at glancing x-ray incidence. The spectra are scaled

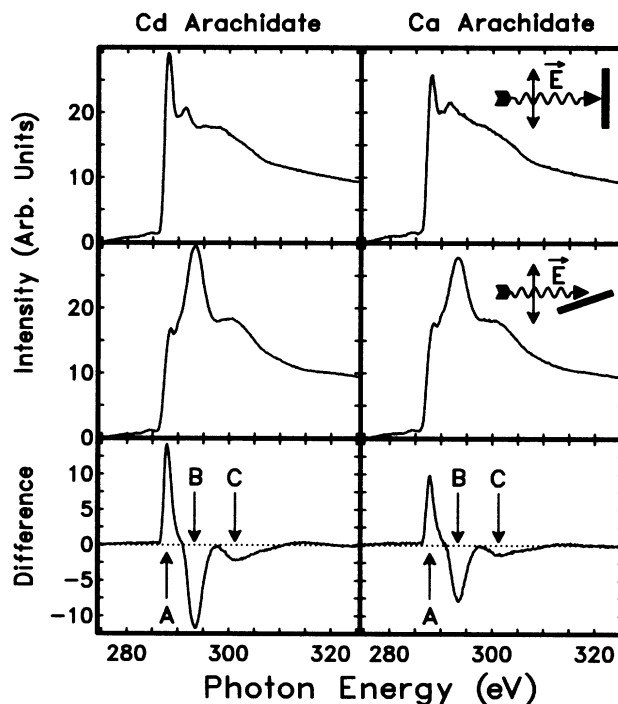


FIG. 1. Comparison of the angular dependence of films of CdA and CaA on a Si(111) surface. The top two rows show the spectra taken at x-ray incidence angles of $\theta = 90^\circ$ and $\theta = 20^\circ$, respectively. The bottom row shows the result of subtracting the glancing-incidence spectra from the normal-incidence spectra. This reveals three angle-dependent resonances A, B, and C.

to the same edge jump by our matching their intensities at 275 and 320 eV. The bottom row shows the result of subtracting the glancing- from the normal-incidence spectra. This clearly isolates three angle-dependent resonances *A*–*C* of which resonance *A* has the opposite angular dependence as compared with resonances *B* and *C*. Also, CdA is seen to exhibit a greater angular dependence than CaA.

In order to determine the LB chain orientation from the angular dependence of the spectra, we have to assign the NEXAFS resonances to transitions to specific molecular-orbital final states. The assignment of resonances follows from previous *K*-shell excitation studies of linear¹⁰ and cyclic¹¹ free and condensed hydrocarbons and the NEXAFS spectrum of polyethylene.¹² Resonance *A* corresponds to transitions to C-H antibonding orbitals and has maximum intensity when **E** lies in the plane of the CH₂ bonds, i.e., perpendicular to the chain direction. Resonance *B* is a C-C σ resonance¹³ which exhibits its largest intensity for **E** along the C—C bonds. For a saturated chain with a C—C—C bond angle of 115°,¹⁴ the largest intensity is expected for **E** along the chain direction as previously discussed for polyethylene.¹² The origin of the weaker resonance *C* will be discussed below. Qualitatively, the CdA and to a lesser degree the CaA chains must be oriented perpendicular to the surface since the C-H resonance is strongest for **E** parallel to the surface and the C-C resonance perpendicular to the surface.

The accurate orientation of the chains on the surface was determined from the intensities of peaks *A*–*C* in NEXAFS spectra measured as a function of **E** orientation in 10° intervals. The NEXAFS spectra were fitted with a superposition of a Gaussian-broadened step function, Gaussians for peaks *A* and *B*, and an asymmetric Gaussian function for peak *C*, as discussed in detail elsewhere.¹⁵ The functions and parameters for the individual peaks provided a good fit to all spectra, independent of angle and sample. The results of the fits for CdA are shown in Fig. 2. Resonance *A*, which is associated with transitions to C-H antibonding orbitals, exhibits the opposite angular dependence as compared with resonance *B* which corresponds to C-C σ^* final states. The fact that the angular dependence of peaks *B* and *C* is identical leads us to assign resonance *C* to transitions to C-C σ^* orbitals which are higher in energy than those associated with resonance *B*. Figure 2 also compares the measured intensity distributions with those calculated for various tilt angles of the macroscopic chain direction from the surface normal. Here we have assumed that the measured C-C resonance intensity arises from a superposition of local C-C σ^* orbitals which are tilted relative to

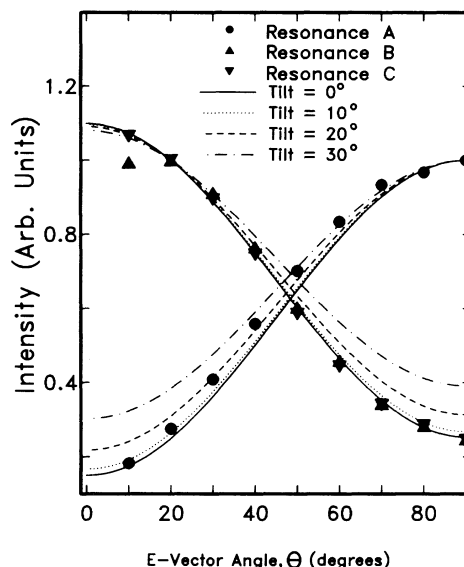


FIG. 2. Intensities of resonances *A* (circles), *B* (upright triangles), and *C* (inverted triangles) determined from fits of the original CdA NEXAFS spectra and theoretical fits as a function of the tilt angle of the macroscopic chain direction from the surface normal.

each other by the C—C—C bond angle of 115°. From this comparison we conclude that the CdA chains are oriented normal to the surface with an uncertainty of $\pm 15^\circ$. Our results for CdA are in good agreement with the vertical chain orientation found in CdA multilayers on silver and silver bromide substrates.¹⁶

The rather large uncertainty of the *absolute* tilt-angle determination from the fit of the original data has led us to use a different approach in determining the difference between the Cd and Ca arachidate orientations. The *relative* orientation of CaA with respect to CdA is most accurately determined by analysis of difference spectra as shown at the bottom of Fig. 1. This method removes all isotropic components in the NEXAFS spectra including the effects of incomplete x-ray polarization. In our analysis, the spectrum recorded at $\theta=50^\circ$ was subtracted from all others for both CaA and CdA. Peaks *A*–*C* in the difference spectra (see Fig. 1) were then fitted with the same functions, energy positions, and widths as those used for fitting the original data, and the intensities resulting from the fits are plotted in Fig. 3. The angular dependence of the experimental data points in Fig. 3 was fitted with a theoretical curve (solid and dashed lines) to determine the relative chain orientations. For resonances *A*, we used the theoretical expressions describing the angular dependence of the C-H resonances,

$$I^{C-H}(\tau) = A \left[1 - \frac{3}{4} (1 - \cos 2\tau + \cos \gamma_{HCH} - \cos 2\tau \cos \gamma_{HCH}) \right] [\cos^2 \theta - \cos^2 50^\circ], \quad (1)$$

where τ is the tilt angle of the chain from the surface normal, A is a scaling constant which, for a given resonance, is

the same for CdA and CaA, and $\gamma_{\text{HCH}} = 110^\circ$ is the H—C—H bond angle. Equation (1) is derived under the assumption that the C-H resonance originates from transitions to C-H antibonding orbitals which lie in the H-C-H plane.¹² The data points for resonances B and C are fitted with the theoretical intensity distribution for the C-C σ resonances,

$$I^{C-C}(\tau) = B[1 - \frac{1}{4}(1 + \cos\gamma_{\text{CCC}}\cos 2\tau)][\cos^2\theta - \cos^2 50^\circ], \quad (2)$$

where B is a scaling constant and $\gamma_{\text{CCC}} = 115^\circ$ is the C—C—C bond angle. For Eqs. (1) and (2) we have assumed that the chains tilt in the plane of the C—C—C bonds and that an average over domains eliminates any azimuthal dependence. Using CdA as our reference system and assuming that the chains are aligned normal to the surface, we can compare the angular dependence of the respective resonances for CdA and CaA in Fig. 3. We deduce a tilt angle $\tau = 32.8 \pm 5^\circ$ of the CaA chain from the surface normal using resonance A and $\tau = 33.8 \pm 5^\circ$ using both resonances B and C.

There is a simple geometric argument which can account for the stability of these two orientations. Adjacent hydrocarbon chains can interlock "in phase" at certain tilt angles. This condition is fulfilled for an upright chain orientation on the surface, and again when the chain has tilted to allow slippage of adjacent chains by multiples of the chain period R . Figure 4 shows that this is satisfied when

$$\tan\tau = nR/D, \quad n=0,1,2,\dots, \quad (3)$$

where τ is the tilt of the hydrocarbon chain from the surface normal, R is the periodicity of the chain, i.e., the distance between second-nearest-neighbor carbon atoms

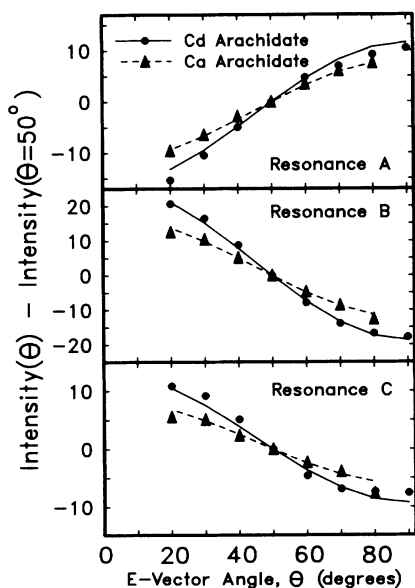


FIG. 3. Intensities of peaks A–C in the difference spectra of CdA, obtained by subtraction of the spectrum for $\theta = 50^\circ$ from the spectrum at each θ , compared with the intensities of the same peaks of CaA. Also shown are fits of the data points by Eqs. (1) and (2).

($R = 2.52 \text{ \AA}$), and D is the minimum separation between hydrocarbon chains. If the chains are vertical ($\tau = 0^\circ$ and $n = 0$), Eq. (3) is satisfied for any separation D . If the chains are tilted, however, then crowding between the chains becomes important and only certain angles are allowed. For example, the minimum separation typically allowed between carbon atoms in adjacent organic molecules is $D = 3.6$ to 4.0 \AA .¹⁷ This yields a tilt angle of 32° to 35° with use of Eq. (3), which is excellent agreement with the $33^\circ \pm 5^\circ$ tilt angle determined for Ca arachidate. Thus, Cd and Ca arachidate satisfy Eq. (3) with values of $n = 0$ and 1 , respectively.

Figure 4 suggests that CdA with its vertical chain is bonded to the surface with only *one* oxygen atom, while CaA with its tilted chain is almost perfectly chelated with both oxygens on the surface. The bidentate surface bond may additionally stabilize the 33° tilted configuration observed for CaA. It is not clear, however, what role the cation plays in the surface bond. Both cations are in $+2$ oxidation states and are approximately the same size, as estimated from the metal-oxygen nearest-neighbor distances in crystalline CaO and CdO which are 2.405 and 2.347 \AA , respectively.¹⁸ It is possible that the main reason for the different orientations lies in the conditions during the transfer of the films, e.g., the pH of the solutions. Whatever the reason, our results establish that certain molecular orientations on the surface are

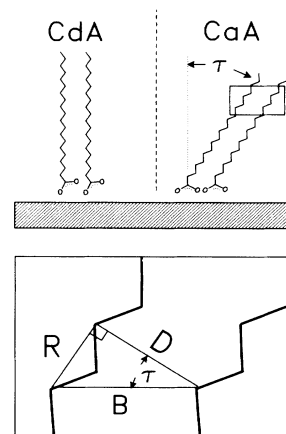


FIG. 4. Packing of hydrocarbon chains and quantum tilt model. Proposed models for the hydrocarbon chain orientation in films of CdA and CaA. The CdA chains are normal to the surface, while the CaA chains are tilted by 33° . At the bottom it is shown how the efficient packing of the chains with periodicity R depends upon the tilt angle τ and minimum separation D between chains.

avored by the in-phase interlocking of adjacent chains. More generally, the present study demonstrates the power of the NEXAFS technique to investigate the orientation and structure of thin organic films on surfaces.

We would like to thank B. Hermsmeier, P. Stevens, and J. Solomon for help with the measurements. This work was done at the Stanford Synchrotron Radiation Laboratory which is supported by the Office of Basic Energy Sciences of the Department of Energy and the Division of Materials Research of the National Science Foundation.

¹See *Thin Solid Films* **132–134** (1985).

²G. L. Gaines, Jr., *Insoluble Monolayers at Liquid-Gas Interfaces* (Wiley-Interscience, New York, 1966), Chap. 8.

³M. Pomerantz, F. H. Dacol, and A. Segmüller, *Phys. Rev. Lett.* **40**, 246 (1978).

⁴S. Garoff, H. W. Deckman, J. H. Dunsmuir, M. S. Alvarez, and J. M. Bloch, *J. Phys. (Paris)* **47**, 701 (1986).

⁵F. Kimura, J. Umemura, and T. Takenaka, *Langmuir* **2**, 96 (1986).

⁶J. P. Rabe, J. D. Swalen, and J. F. Rabolt, *J. Chem. Phys.* **86**, 1601 (1987).

⁷D. P. E. Smith, A. Bryan, C. Quate, J. Rabe, Ch. Gerber,

and J. D. Swalen, *Proc. Natl. Acad. Sci. USA* **84**, 969 (1987).

⁸J. Stöhr and R. Jaeger, *Phys. Rev. B* **26**, 4111 (1982); J. Stöhr, *Z. Phys. B* **61**, 439 (1985).

⁹The spectrum of CdA has been published before as part of an overview of NEXAFS spectroscopy [J. Stöhr and D. A. Outka, *J. Vac. Sci. Technol. A* **5**, 919 (1987)] but no detailed analysis was presented.

¹⁰A. P. Hitchcock and I. Ishii, *J. Electron Spectrosc. Relat. Phenom.* **42**, 11 (1987).

¹¹A. P. Hitchcock, D. C. Newbury, I. Ishii, J. Stöhr, J. A. Horsley, R. D. Redwing, A. L. Johnson, and F. Sette, *J. Chem. Phys.* **85**, 4849 (1986).

¹²J. Stöhr, D. A. Outka, K. Baberschke, D. Arvanitis, and J. A. Horsley, *Phys. Rev. B* **36**, 2967 (1987).

¹³F. Sette, J. Stöhr, and A. P. Hitchcock, *J. Chem. Phys.* **81**, 4906 (1984).

¹⁴The C–C–C bond angles of a long hydrocarbon chain molecule are typically somewhat larger than the ideal tetrahedral angle of 109.5°. For example, in the structure of potassium palmitate the average angle is 114.4°: J. H. Dumbleton and T. R. Lomer, *Acta Cryst.* **19**, 301 (1965).

¹⁵D. A. Outka, J. Stöhr, J. P. Rabe, and J. Swalen, *J. Chem. Phys.* (to be published).

¹⁶J. F. Rabolt, F. C. Burns, N. E. Schlotter, and J. D. Swalen, *J. Chem. Phys.* **78**, 946 (1983).

¹⁷C. W. Bunn, *J. Chem. Soc. Trans. Faraday Soc.* **35**, 482 (1939).

¹⁸R. W. G. Wyckoff, *Crystal Structures* (Wiley-Interscience, New York, 1966), Vol. 1.